Tensile creep of a structural epoxy adhesive: Experimental and analytical characterization

Inês Costa *, Joaquim Barros

ISISE—University of Minho Department of Civil Engineering, Campus de Azurém, 4800-058 Guimarães, Portugal

A B S T R A C T

Epoxy adhesives are nowadays being extensively used in Civil Engineering applications, mostly in the scope of the rehabilitation of reinforced concrete (RC) structures. In this context, epoxy adhesives are used to provide adequate stress transference from fibre reinforced polymers (FRP) to the surrounding concrete substrate. Most recently, the possibility of using prestressed FRPs bonded with these epoxy adhesives is also being explored in order to maximize the potentialities of this strengthening approach. In this context, the understanding of the long term behaviour of the involved materials becomes essential. Even when non-prestressed FRPs are used a certain amount of stress is permanently applied on the adhesive interface during the serviceability conditions of the strengthened structure, and the creep of the adhesive may cause a continuous variation in the deformational response of the element. In this context, this paper presents a study aiming to experimentally characterize the tensile creep behaviour of an epoxy-based adhesive currently used in the strengthening of concrete structures with carbon FRP (CFRP) systems. To analytically describe the tensile creep behaviour, the modified Burgers model was fitted to the experimental creep curves, and the obtained results revealed that this model is capable of predicting with very good accuracy the long term behaviour of this material up to a sustained stress level of 60% of the adhesive's tensile strength.

© 2015 Elsevier Ltd. All rights reserved.

1. Introduction

One of the most common uses of fibre reinforced polymers (FRP) in Civil Engineering applications is in the scope of rehabilitation and strengthening of reinforced concrete (RC) structures. For that purpose, the FRPs, in the form of sheets, laminates or bars, are bonded to the existing structures by means of an adhesive. The research group at Minho University has already applied these FRPs externally (externally bonded reinforcement - EBR), near surface mounted (NSM) [1] or even embedded through-section (ETS) [2]. The installation of NSM-FRPs is able of increasing the load carrying capacity of a structural element with minor aesthetical impact and negligible structural weight increase, among a number of other advantages as referred by De Lorenzis and Teng [3]. Most recently, in order to take advantage of the high tensile strength of the FRP, the possibility of applying FRPs with a certain prestress is being further explored for increasing the load carrying capacity of a strengthened element at serviceability limit state conditions [4–5].

Generally, the effectiveness of these strengthening systems is, in a first phase, evaluated by means of monotonic tests, meaning that a model of the structural system is constructed and loaded up to failure. However, this type of characterization only provides the maximum expectable strength and not the real deformational behaviour of the strengthening system during the working life of the structure.

Mainly motivated by the interest of using prestressed NSM-FRPs (Fig. 1), the knowledge of the long term deformability of the intervening materials becomes essential. The creep of structural adhesives is already recognized to be a material property of major importance to guarantee adequate stress transfer between the FRP and surrounding material over time. In fact, Quantrill and Hollaway, Nordin and Täljsten and Wang et al. have already exposed that this property plays an important role on the long term efficacy of the strengthening system [6–8]. However, the investigation in this area is scarce, despite the potentially negative effects the creep behaviour of adhesives can have in terms of the strengthening effectiveness of a FRP-based system.

Creep, usually defined as the increase of deformation over time under sustained stress, is recognized to be a relevant phenomenon when dealing with adhesives, and ISO and ASTM already define the methods to assess this property [9–10]. Additionally, the analysed specialized bibliography on this topic revealed that the mechanical performance of adhesives changes in fact with time, mainly due to the level of applied stress, but also due to environmental conditions such as temperature and humidity, as referred by ASTM, Dean and Feng et al. [10–12].

* Corresponding author. Tel.: +351 252 315 199.
E-mail addresses: inescosta@civitest.com (I. Costa),
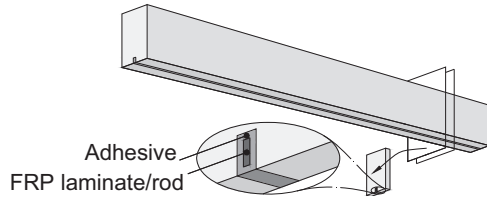barros@civil.uminho.pt (J. Barros).

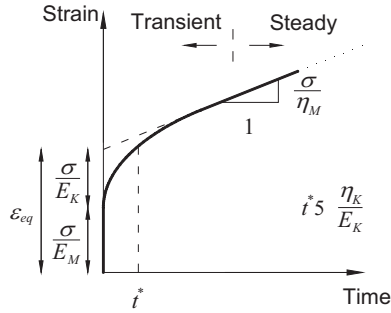**Fig. 1.** Representation of a NSM-FRP application on a RC beam.

Fig. 2. Strain evolution with time in Burgers Model.

The creep behaviour of adhesives is frequently modelled using rheological models and is usually illustrated by means of Hookean springs and Newtonian dashpots that replicate, respectively, the elastic and viscous components of the material's behaviour (Brinson and Brinson, [13]). Burgers model, depicted in Fig. 2, is the most common and generalist creep model. This model is able of describing the time-strain variation of most of the existing epoxy-based adhesives, and will therefore be taken as reference to describe the behaviour of the adhesive adopted in the present research programme. This model is simulated by the following equation:

$$\varepsilon_{creep}(t) = \frac{\sigma}{E_M} + \frac{\sigma}{\eta_M}t + \frac{\sigma}{E_K}\left(1 - \exp\left(-\frac{E_K}{\eta_K}t\right)\right) \tag{1}$$

where $\varepsilon_{creep}(t)$ is the strain evaluated at a certain time instant t, σ is the applied stress, E_M and η_M are Maxwell's elastic modulus and coefficient of dynamic velocity, E_K and η_K are Kelvin's elastic modulus and coefficient of dynamic velocity.

Feng et al. [12] suggested that the tensile creep strain, $\varepsilon_{creep}(t, T)$ can be estimated by the exponential function shown in Eq. 2, which was re-written to improve the resemblance with the rheological model that will be afterwards reported in the present document

$$\varepsilon(t, T) = \frac{\sigma_0}{E_0} + \sigma_0\left(\frac{1}{E_e} - \frac{1}{E_0}\right)\left(1 - e^{-(t/t^*)^{1-n}}\right) \tag{2}$$

where σ_0 is the applied stress level, E_0 the initial Young modulus, E_e is the equilibrium modulus given in Eq. 3, t^* is the retardation time and n is a coupling parameter related to moisture absorption

$$E_e = 2G_r(1+\nu) \tag{3}$$

where G_r is the rubbery plateau shear modulus and ν is Poisson's ratio ($\nu = 0.5$ since the material is in the rubbery state).

The unique feature of this model is related to the n parameter, whose value is basically related to the activation energy of the molecular motion. If a specimen is saturated, the presence of moisture enhances the molecular mobility and, therefore, decreases the amount of activation energy required, resulting in lower values of n. As reference, it can be mentioned that Feng et al. [12] obtained in their tests an initial Young modulus, E_0, of 2.5 GPa, retardation times, t^*, ranging between 54 and 16204 days and values of n ranging from 0.51 to 0.73 for varying degrees of relative humidity.

In another paper, Majda and Skrodzewicz [14] proposed a model purely based on Burgers Model (Eqs. (4) and (5)). The singularity

recognized in this paper is the suggestion that the coefficients of dynamic viscosity, η_0 and η_1, are primarily dependent on the applied stress (see Eqs. (6) and (7)). Additionally, the elastic modulus of the relaxation response, herein designated as E_1, was also defined as a function of the applied stress (Eq. (8))

$$\varepsilon(t, T) = \frac{\sigma_0}{E_0} + \frac{\sigma_0}{\eta_0}t + \frac{\sigma_0}{E_1}\left(1 - e^{-t/t^*}\right) \tag{4}$$

$$t^* = \frac{\eta_1}{E_1} \tag{5}$$

$$\eta_0(\sigma_0) = e^{a_1 - a_2\sigma_0} \tag{6}$$

$$\eta_1(\sigma_0) = e^{a_3 - a_4\sigma_0} \tag{7}$$

$$E_1(\sigma_0) = a_5\sigma_0^2 - a_6\sigma_0 + a_7 \tag{8}$$

As an indication, Majda and Skrodzewicz [14] obtained an initial elastic modulus, E_0, of 2.323 GPa and retardation times, t^*, of 3–24 min. Note that this last value is exceptionally lower when compared to the one obtained by Feng et al. [12].

Taking into account the information previously exposed, and in order to address the lack of research in this topic, an experimental programme was carried out aiming the assessment of the tensile creep behaviour of an epoxy-based structural adhesive, traded under the commercial name "S&P Resin 220 epoxy adhesive", used in a commercial NSM-CFRP (carbon FRP) system. According to the material safety sheet, the epoxy resin solution is composed of bisphenol A and neopentyl glycol diglycidyl ether while the hardener contains poly(oxypropylene)diamine, triethylentetramine, piperazine and aminoethylpiperazine. For that purpose, nine dumbbell-shaped samples of adhesive were tested under three different load levels. Later, a modified Burgers equation was used to model the creep strain curves obtained, as well as the corresponding creep modulus curves.

2. Material characterization

In the first phase of the experimental programme the instantaneous properties of the epoxy adhesive to be tested under tensile creep were evaluated. For this purpose dumbbell-shaped specimens of adhesive were prepared observing ISO 527-2 recommendations [15]. According to this standard, the effective cross section under tensile stress should be 10×4 mm^2. Note that these dimensions are representative of the thickness of the adhesive layer used in the NSM-CFRP strengthening technique for bonding the CFRP reinforcement to the surrounding concrete. In the prestressed NSM-CFRP technique developed in the research project that the present work is part of it, a thickness of about 3 mm was adopted. To maintain the constituents of the adhesive at 20 °C and 60% of relative humidity while manufacturing the specimens, the containers of the constituents were transported to a climatic chamber 24 h prior the moulding process of the specimens. The epoxy adhesive analysed is a bi-component material that, according to the supplier, should be mixed in a proportion of 1:4 (in weight). After weighting both components in the recommended ratio, the mixture was performed manually inside a bowl and using a spatula, as it would be in a real case application, and at room temperature. After obtaining a uniform colour, the mixture was poured into a silicon mould, and no efforts were made to remove air bubbles, in order to produce a final product that is in every way similar to the one obtained in an actual application. After moulding, all the specimens to be tested were again transported to the climatic chamber until the curing time was over. When the specimens were removed from the mould, the edges were gently scraped in order to remove occasional sharp edges. For the measurement of the strain during the test, a control
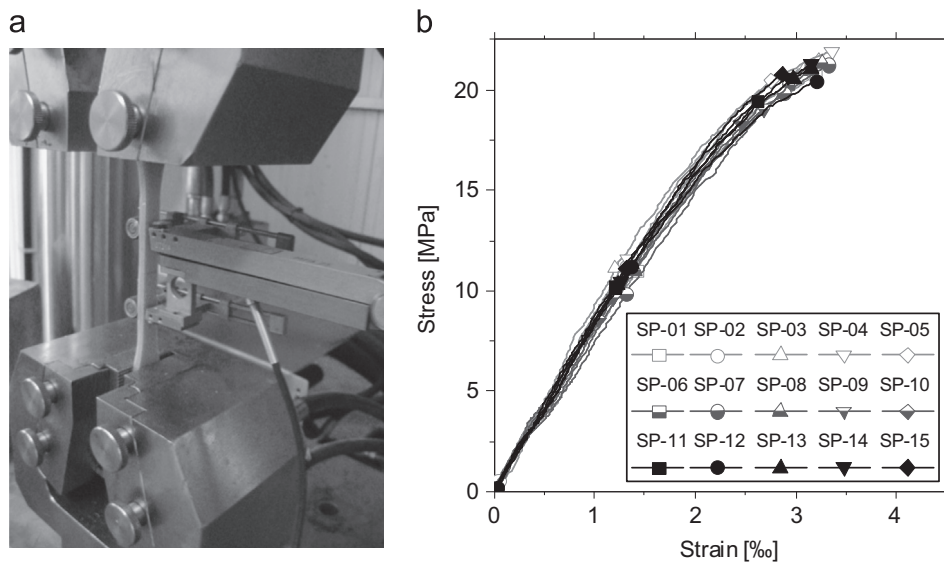
Fig. 3. Tensile tests: (a) test setup and (b) stress versus strain curves.

Table 1
Instantaneous properties of the epoxy adhesives.

Specimen	Curing time [days]	E_a [GPa]	r^2	f_a [MPa]	ε_a [‰]
SP-01	2	7.53	0.9961	20.9	3.20
SP-02		7.41	0.9916	20.8	3.07
SP-03		7.47	0.9901	21.4	3.22
SP-04		7.67	0.9949	21.9	3.36
SP-05		7.86	0.9983	20.5	2.76
Average		7.59 (0.18) {2%}	–	21.1 (0.6) {3%}	3.12 (0.23) {7%}
SP-06	3	7.37	0.9958	21.2	3.14
SP-07		7.32	0.9977	21.3	3.32
SP-08		7.39	0.9961	21.3	3.26
SP-09		7.19	0.9934	19.0	2.69
SP-10		6.99	0.9978	18.4	2.46
Average		7.25 (0.17) {2%}	–	20.2 (1.4) {7%}	2.97 (0.38) {13%}
SP-11	7	7.42	0.9952	19.5	2.62
SP-12		7.00	0.9942	20.5	3.20
SP-13		7.47	0.9948	21.1	3.15
SP-14		7.40	0.9959	21.3	3.15
SP-15		7.83	0.9955	20.8	2.87
Average		7.42 (0.29) {4%}	–	20.6 (0.7) {3%}	3.00 (0.25) {8%}

r^2 is the coefficient of determination of the linear regression of the stress versus strain curve.
Average (Standard deviation) {Coefficient of variation}

length of 50 mm was adopted, as recommended by ISO 527-2, and the tensile test was performed under displacement control at a rate of 2 mm/min. Although the recommended curing time for this particular adhesive is 7 days, it was observed that after 2 days, in terms of tensile strength, f_a, and elastic modulus, E_a, the instantaneous properties were already stabilized (see Fig. 3 and Table 1). Moreover, the data sheet of this adhesive reports that three days after application, it exhibits adequate bond strength to concrete. For that reason, the curing time adopted for the creep specimens was reduced from 7 days to 3 days.

3. Tensile creep

The assessment of the tensile creep properties of the adhesive was performed in a mechanical creep table, schematically represented in Fig. 4. Three series of specimens were prepared, and each one was made from a batch of adhesive mixed exactly 3 days prior to creep load application, always using the same container of material. All specimens were produced and stored following the same protocol

detailed in Section 2 and the creep tests were performed in a climatic chamber programed to maintain a constant temperature of 20 °C and 60% of relative humidity. Each batch of adhesive produced 14 specimens: 5 for material testing at time of loading (72 h of age, herein labelled as $t = 0$ h), 5 for material testing at the end of the creep test (1072 h of age, herein labelled as $t = 1000$ h) and 4 for creep testing (3 for tensile creep test and 1 for control purposes).

Each creep specimen was instrumented with two strain-gauges type BFLA-2-3-3 L from TML, with a 2 mm measuring length installed precisely at the geometric centre of each face (see Fig. 5a). The reference specimen was also instrumented, but in this case with only one strain gauge to measure any possible environmental effects on the material, on the strain gauges wires, as well as other unexpected fluctuations in the readings. Although it is acknowledged that the applied strain gauge has a rather small size, due to the small grain size of the particles that compose the adhesive, the monitored section is believed to be sufficiently representative of the tensile strain field installed in the adhesive. In each series, three different load levels were applied, corresponding to approximately 20%, 40% and 60% of the adhesive's tensile
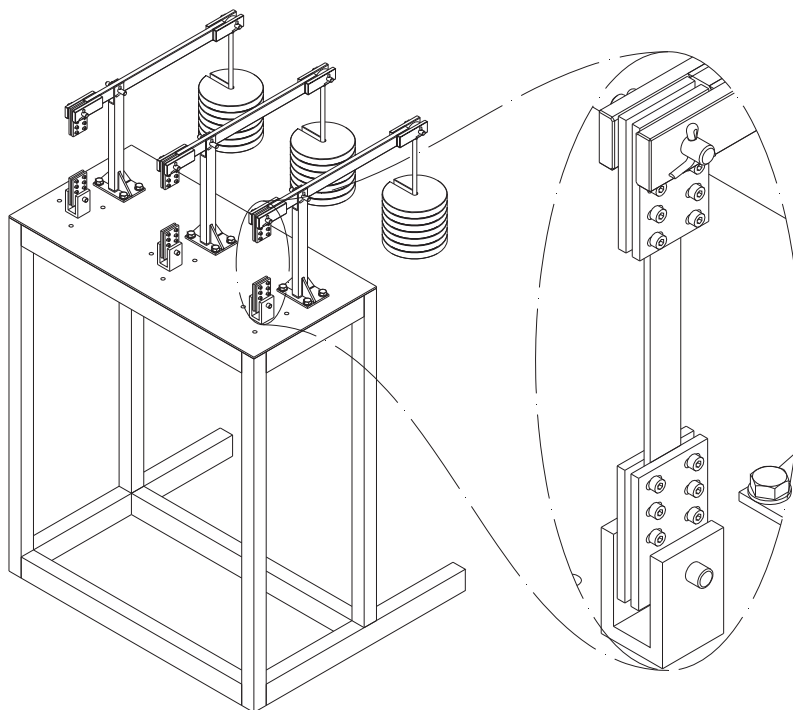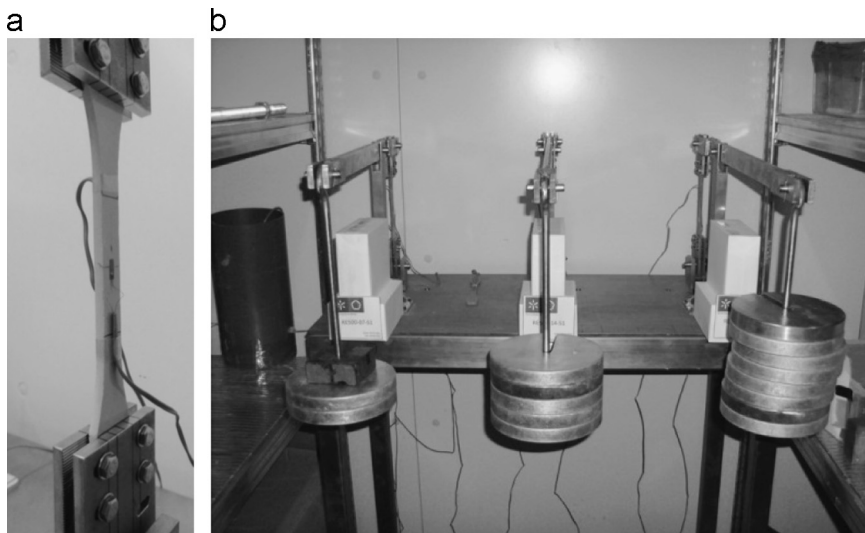
Fig. 4. Mechanical creep table.

Fig. 5. Tensile creep tests: (a) specimens installation and (b) specimens under sustained load.

Table 2
Instantaneous properties of the creep specimens at time of loading and after 1000 h.

Series	Age of the adhesive container *	$t=0$ h		$t=1000$ h		ΔE_a[%]	Δf_a[%]
		E_a [GPa]	f_a [MPa]	E_a [GPa]	f_a [MPa]		
I	$\approx$ 9 days	7.70 (0.16) {2%}	20.2 (2.2) {11%}	7.61 (0.29) {4%}	20.9 (1.3) {6%}	−1.1	3.3
II	$\approx$ 69 days	6.79 (0.41) {6%}	20.3 (1.7) {8%}	6.36 (0.29) {5%}	17.7 (1.6) {9%}	−6.4	−13.2
III	$\approx$ 124 days	6.72 (0.74) {11%}	15.0 (2.5) {16%}	7.36 (0.84) {11%}	15.7 (5.4) {35%}	9.6	4.5

* Refers to the time between the reception of the adhesive container and the mixture of components.
Average (Standard deviation) {Coefficient of variation}

$\Delta E_a = (E_{a,t=1000h} - E_{a,t=0h})/E_{a,t=0h}; \Delta f_a = (f_{a,t=1000h} - f_{a,t=0h})/f_{a,t=0h}$

strength indicated in Table 1 (see Fig. 5b). The evolution of strain under sustained stress was recorded for 1000 h, as recommended by ISO and ASTM [9,10].

Table 2 summarizes the average instantaneous properties determined on the specimens of the three series, and the corresponding stress–strain curves are depicted in Fig. 6. In most cases, the obtained
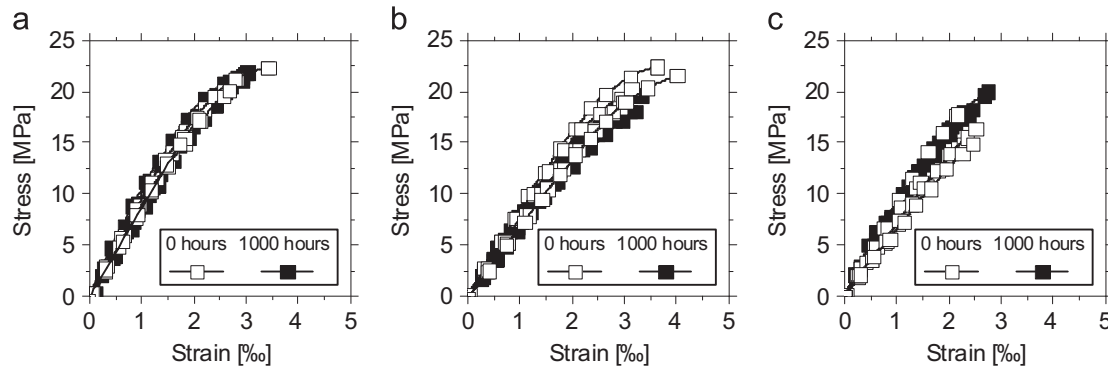
Fig. 6. Control tensile tests: (a) Series I, (b) Series II and (c) Series III.
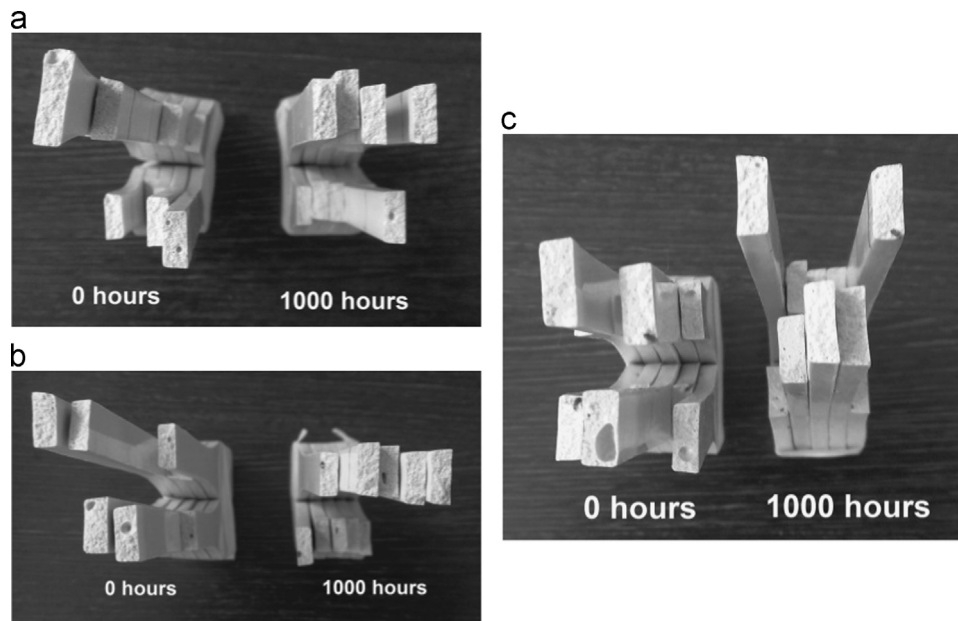

Fig. 7. Failure surface of the tensile specimens: (a) Series I, (b) Series II and (c) Series III.

properties were relatively close to the ones presented in Table 1. However, in Series III, the specimens exhibited an abnormally low tensile strength both at $t=0$ h and $t=1000$ h. This fact may be due either to a deficient mixture of the components, although no significant increase in porosity was observed in the failure surface between series of specimens, or eventually to the approaching of the expiration date of the material. In reality, the creep parameters presented later, in Section 3.2, suggest that during the execution of this experimental programme, some type of aging process might have occurred and additional tests will be carried out in due time to investigate the causes of this material degradation. Note that according to Fig. 7, Series III specimens tested at 1000 h, exhibit less voids than the specimens tested at 0 h, even though both exhibit similar tensile strength and elastic modulus according to Table 2.

Regarding the tensile creep tests, load was applied in the specimens in approximately 3–5 s using steel plates. The effective load, W, applied in the creep specimens is presented in Table 3, as well as the effective applied stress, σ, that was calculated by applying the following equation:

$$\sigma = \frac{Wg\varphi}{A} \qquad (9)$$

where W is the mass at the loaded end of the lever, g is the gravitational acceleration, φ ($=3$) is the amplification factor of the creep table and A is the cross sectional area of the tested specimen.

Table 3
Geometric properties of the specimens.

Series	Specimen	W [kg]	A [mm²]	σ [MPa]	% $f_{max,0\,h}$ [%]	% $f_{1000\,h}$ [%]
I	S1_A	6	43.486	4.32	21	21
	S1_B	11	43.278	7.81	39	37
	S1_C	17	43.067	11.94	59	57
II	S2_A	6	41.272	4.55	22	26
	S2_B	11	42.494	7.95	39	45
	S2_C	17	45.296	11.35	56	64
III	S3_A	6	42.003	4.47	30	28
	S3_B	11	41.763	8.09	54	51
	S3_C	17	43.487	11.82	79	75

The creep apparatus used magnifies the applied dead weight in 3 times meaning that $\varphi=3$.

$\% f_{max,0h} = \sigma/f_{a,0h}$ and $\% f_{0h} = \sigma/f_{a,1000h}$

In order to standardize the load application process, three load levels were defined for all three series of specimens, taking into account the geometry of the specimens and the creep table configuration. This resulted in the definition of the following mass levels: 6 kg, 11 kg and 17 kg, herein labelled as A, B and C, respectively. As in Series III the control tensile tests revealed a lower tensile strength, the effective percentage of applied stress was different from the predefined level.
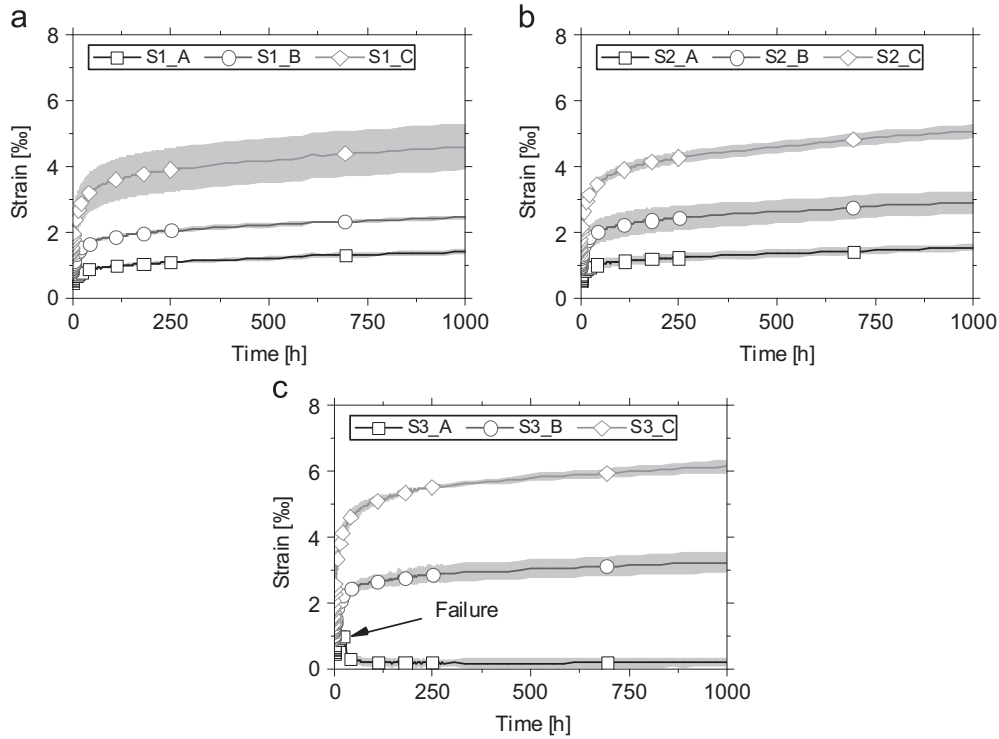
Fig. 8. Strains versus time: (a) Series I, (b) Series II and (c) Series III.

3.1. Experimental results

After monitoring the specimens for the required period of time, the creep strain curves were constructed. It is worth noting that the reference creep specimens did not exhibit significant strain variation over time and, therefore, the data obtained from the loaded specimens was directly used [3]. The envelope of the time versus strains recorded in the monitored faces is plotted in Fig. 8, as well as the corresponding average strain, showing that in terms of shape of the creep strain curve all specimens exhibited similar time dependent variation. The largest difference between opposing strain gauges was observed in Series I, where the difference of strains was larger than 1‰ in Specimen C. In the remaining specimens, the difference of strains over time between opposing strain gauges was fairly similar in all cases. It is believed that this dispersion of strains is related to the heterogeneity of the adhesive mixture, caused by the manual mixing process and the subjectivity of the "uniform colour" criterion, as well as to the small size of the strain gauge reference length (2 mm), which may cause the reading of strains in zones with relatively different properties. It is also noteworthy that, after 1000 h of loading, the adhesive specimens loaded with 12 MPa exhibited an average strain of 4.61‰, 5.07‰ and 6.15‰ in Series I, II and III, respectively. However, according to the preliminary tensile tests, the ultimate strain of these samples was only about 3‰ (Table 1). It is also important to notice that Specimen S3_C, depicted in Fig. 5c, fractured at about 27 h after load application, in the vicinity of the top anchorage, possibly due to an accidental shock against the creep table.

3.2. Analytical model

As already suggested in Section 1, the tensile creep behaviour of epoxy adhesives is usually well defined using Burgers equation (Eq. (1)). Observing Fig. 8, it is evident that the behaviour of the tested adhesive is in fact similar to the one initially proposed (see Fig. 2). Therefore, considering the average strain curves obtained for each specimen, the parameters defining Eq. (1) were determined for each of the curves, as follows:

- The initial strain, $\varepsilon_{creep}(t=0)=\varepsilon_M$ is inversely proportional to Maxwell's elastic modulus, E_M. In this case, E_M is given by Eq. (10);
- Maxwell's coefficient of dynamic viscosity is inversely proportional to the slope of the steady-state branch, ε'_M, as given in Eq. (11);
- Kelvin's elastic modulus, E_K, is proportional to the ε-intercept value, ε_{eq}, of the steady-state branch, as defined in Eq. (12);
- Kelvin's coefficient of dynamic viscosity, η_K, is related to the retardation time t^*, which corresponds to the time instant at which 63% of the Kelvin's steady-state strain is attained. This value can be calculated by first isolating Kelvin's terms in Burgers equation, as defined in Eq. (13). Considering the obtained curve, the time necessary to achieve $0.63\varepsilon_K$, where ε_K is given by σ/E_K, can be determined and the coefficient of dynamic viscosity, η_K, can be determined using Eq. (14)

$$E_M = \frac{\sigma}{\varepsilon_M} \tag{10}$$

$$\eta_M = \frac{\sigma}{\varepsilon'_M} \tag{11}$$

$$E_K = \frac{\sigma}{\varepsilon_{eq}-\varepsilon_M} = \frac{\sigma}{\varepsilon_K} \tag{12}$$

$$\varepsilon_K(t) = \varepsilon(t) - \frac{\sigma}{E_M} + \frac{\sigma}{\eta_M}t \tag{13}$$

$$\eta_K = E_K t^* \tag{14}$$

It is worth noting that the steady-state branch was in this case defined as the last third of the creep monitoring interval, i.e., from $t=666.667$ h to $t=1000$ h.

Table 4 summarizes the parameters determined for each of the specimens, while in Fig. 9 the relationship between numerical and experimental strains is presented. Although in the initial and final instants the correlation between values is satisfactory, in a great portion of the monitored interval the strains are not so well predicted. For this reason, a modified expression based on Burgers

Table 4
Experimental creep curve parameters.

Series	Specimen	ε_M [‰]	ε'_M [‰/h]	ε_{eq} [‰]	ε_{eq} [‰]	t^* [h]	E_M [GPa]	η_M [GPa h]	E_K [GPa]	η_K [GPa h]	$MAPE$ [%]
I	S1_A	0.445	4.099e-04	1.011	0.566	26.5	9.71	10545	7.64	202	8
	S1_B	0.789	4.993e-04	1.969	1.180	24.8	9.90	15640	6.62	164	9
	S1_C	1.282	8.891e-04	3.750	2.468	21.8	9.31	13425	4.84	105	10
II	S2_A	0.511	3.770e-04	1.168	0.657	19.6	8.91	12079	6.93	137	10
	S2_B	0.888	6.117e-04	2.321	1.433	19.8	8.96	13001	5.55	109	10
	S2_C	1.304	1.035e-03	4.080	2.776	19.7	8.71	10964	4.09	81	12
III	S3_A	0.466	–	–	–	–	9.61	–	–	–	–
	S3_B	0.898	3.938e-04	2.850	1.952	19.0	9.02	20547	4.14	77	13
	S3_C	1.363	6.673e-04	5.499	4.136	18.8	8.67	17714	2.86	54	14

$MAPE = \frac{100\%}{N} \sum_{i=1}^{N} \left| \frac{\varepsilon_{exp,i} - \varepsilon_{ana,i}}{\varepsilon_{exp,i}} \right|$ where $\varepsilon_{exp,i}$ and $\varepsilon_{ana,i}$ are the experimental and analytical result of each sampling point i, respectively, and N is the number of sampling points ($N = 487$).
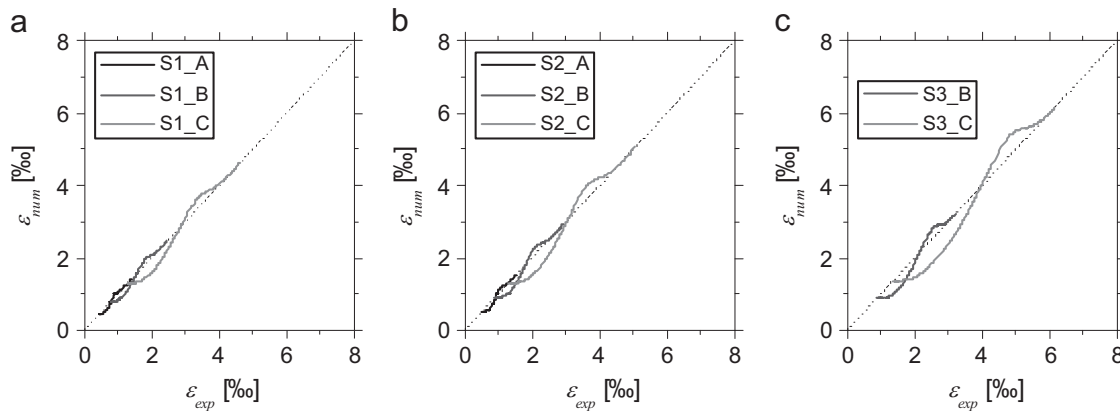
Fig. 9. Burgers model strain versus experimental strain: (a) Series I, (b) Series II and (c) Series III.

model, proposed by Feng et al. [12], was adopted in order to improve the prediction of the experimental strains. The modified equation consists of introducing a new parameter in the original form of Burgers model, n, resulting

$$\varepsilon_{creep}(t) = \frac{\sigma}{E_M} + \frac{\sigma}{\eta_M} t + \frac{\sigma}{E_K} \left(1 - \exp\left(\left(-\frac{E_K}{\eta_K} t \right)^{1-n} \right) \right) \qquad (15)$$

Contrariwise to the previous parameters, the determination of n cannot be performed based on the features of the creep strain curve. Therefore, the parameter n was determined by forcing the slope between experimental and numerical values to be unitary, using the Generalized Reduced Gradient (GRG2) nonlinear optimization, available in Microsoft Excel (2010). The values obtained by this process are fairly constant, as demonstrated in Table 5, and the obtained results reveal that this model is much more accurate, as depicted in Fig. 10.

Up to this point, the obtained parameters represent the best value to predict the behaviour of a single adhesive specimen. However, to validate the applicability of the model, it is necessary to determine at least one set of parameters (E_M, η_M, E_K, η_K and n) per series. Therefore, in Fig. 11, the parameters that are assumed to better describe the mixture of each series are presented.

The value of E_M, depicted in Fig. 11a, was computed as the slope of a linear regression of σ versus ε_M, as defined by the formulation of the model, Eq. (10). Similarly, in Fig. 11b and 11c, η_M and E_K are defined as the slope of σ versus ε'_M and σ versus ε_K, respectively, Eqs. (11) and (12). Regarding the values of η_K and n, it is not possible to define the same type of relationships. For that reason, Fig. 11d and e depicts the values of t^* and n versus the applied stress level.

Of all the linear regressions executed, the one defining E_M is definitely the one leading to better results. E_M is found to exhibit,

Table 5
Modified Burgers equation parameters.

Series	Specimen	n	r^2	$MAPE$[%]
I	S1_A	0.48	0.9984	2
	S1_B	0.48	0.9995	2
	S1_C	0.45	0.9996	2
II	S2_A	0.57	0.9990	1
	S2_B	0.52	0.9995	2
	S2_C	0.49	0.9995	2
III	S3_A	–	–	–
	S3_B	0.53	0.9986	2
	S3_C	0.48	0.9992	3

within each series of specimens, an almost unitary coefficient of determination, r^2, as well as an extremely low coefficient of variation, COV, when all series are taken into account (see Table 6). Moreover, it is worth mentioning that in all cases, E_M is larger than E_a (see Tables 1 and 2), most likely due to the load application speed, which was performed in about 3–5 s, while in the standard tensile tests it would take roughly 12–36 s to achieve the same stress levels. On the other hand, the value of η_M, which also exhibits very good r^2 values within individual series, is not able to produce particularly low COV values when considering all the series ($COV = 25\%$, see Table 6). The same is observed in the determination of E_K, which in general leads to relatively high r^2 (at least 0.9712), but produces a 26% COV when the values of all series are considered.

Lastly, regarding the quantification of t^* and n, the obtained results were somewhat more satisfactory. Apart from the high variability of the retardation time in Series I (see Table 4 and Fig. 11d), the average value of t^* was relatively constant within each series, presenting a 1% COV in Series II and III (Fig. 11d). Note
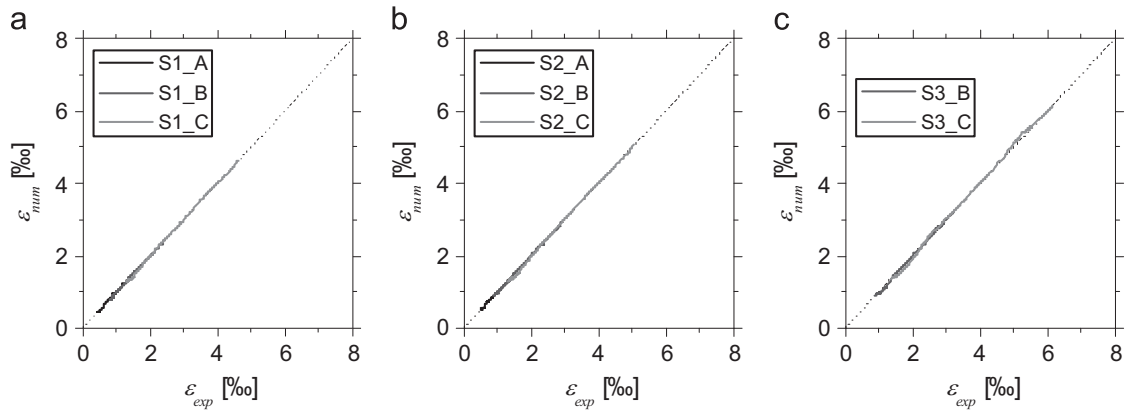
Fig. 10. Modified Burgers model strain versus experimental strain: (a) Series I, (b) Series II and (c) Series III.
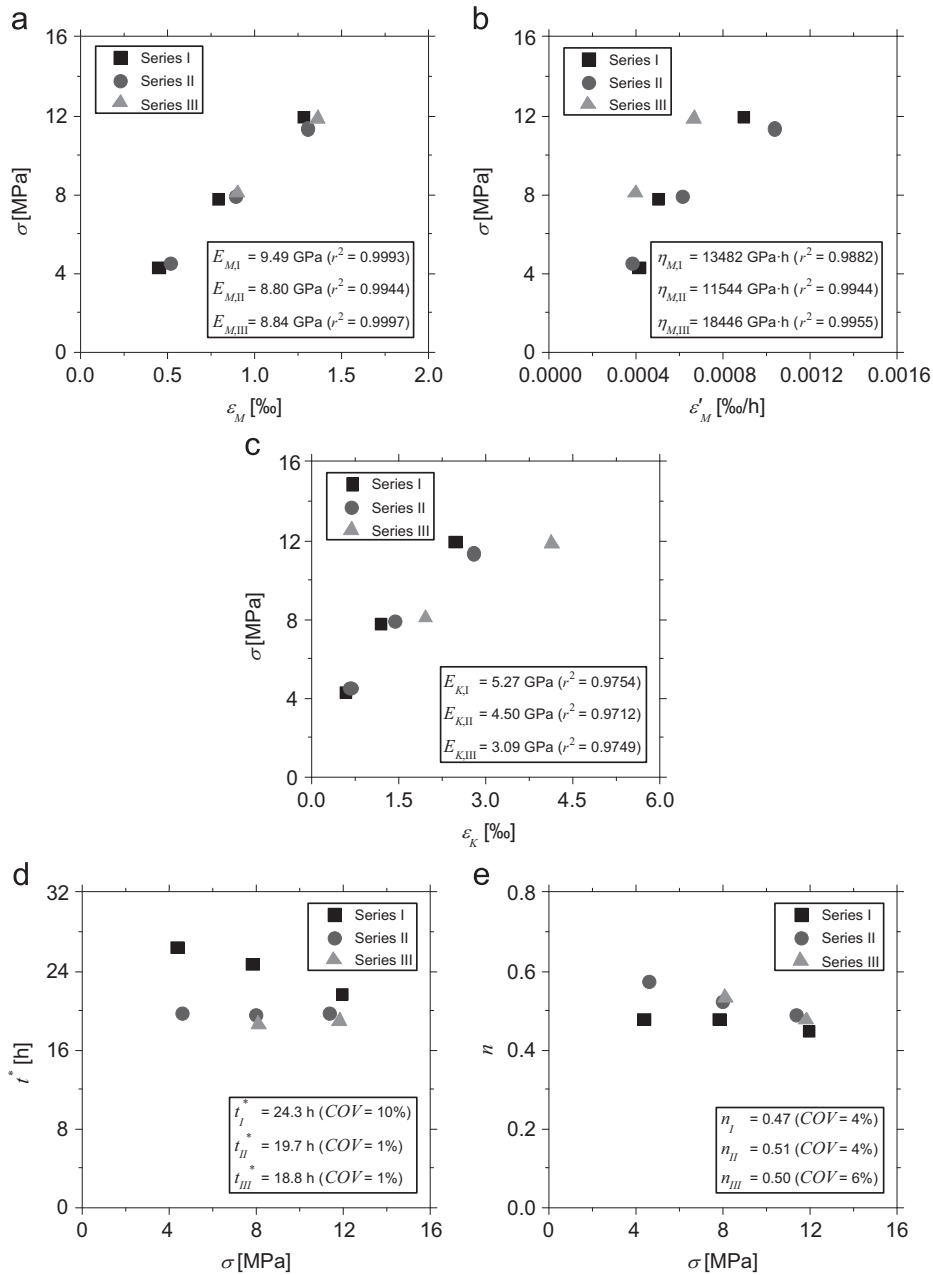

Fig. 11. Modified Burgers model parameters: (a) E_M, (b) η_M, (c) E_K, (d) t^* and (e) n.

Table 6
Average modified Burgers equation parameters of all series tested.

Parameter	E_M [GPa]	η_M [GPa h]	E_K [GPa]	t^* [h]	η_K [GPa h]	n
Series I	9.49	13482	5.27	24.3	128	0.47
Series II	8.80	11544	4.50	19.7	88.7	0.53
Series III	8.84	18446	3.09	18.8	58.1	0.50
Average	9.04 (0.39) {4%}	14491 (3560) {25%}	4.29 (1.10) {26%}	20.9 (3.0) {14%}	91.7 (35.2) {38%}	0.50 (0.03) {6%}

Average (Standard Deviation) {Coefficient of Variation}.
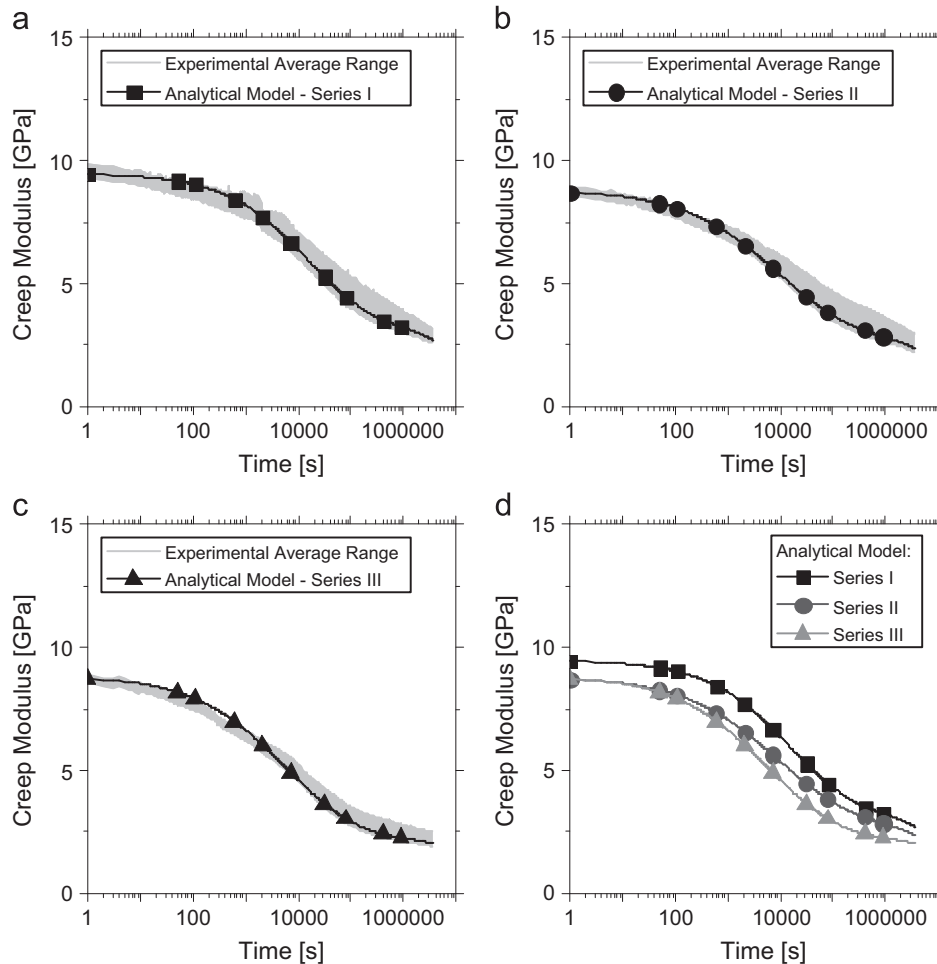
Fig. 12. Creep modulus curves: (a) Series I, (b) Series II, (c) Series III and (d) All analytical creep modulus curves.

that if both E_K and t^* are in fact constant, η_K can also be assumed as constant. Regarding the values of n, the stability of the results is notorious since the COV is never higher than 6% within a series, as reported in Fig. 11e, and it is still 6% when all the specimens are taken into account (see Table 6).

Despite the relatively low number of tests performed, it was noted that some of the parameters have a tendency to decrease with the age of the unmixed components. Taking a closer look at Kelvin's coefficients, E_K and η_K, it was observed that from the first to last series, those parameters are evaluated almost as half of the original value, suggesting that the material may experience an aging effect even before it is mixed.

3.3. Creep curves

One of the main objectives of creep tests is the definition of the creep curves, especially the creep modulus curves. For the specific case of the epoxy adhesive tested, since all the parameters are

approximately constant, it is worth to mention that this proves that this material exhibits linear viscoelastic/viscoplastic tensile behaviour. Therefore, a unique creep modulus curve, $E_{creep}(t)$, can be used to describe the behaviour of the adhesive over time, regardless the applied stress level, which is simulated by the following equation:

$$E_{creep}(t) = \frac{\sigma}{\varepsilon_{creep}(t)} = \frac{1}{\frac{1}{E_M} + \frac{t}{\eta_M} + \frac{1}{E_K}\left(1 - \exp\left(\left(-\frac{E_K}{\eta_K}t\right)^{1-n}\right)\right)} \quad (16)$$

Fig. 12 depicts the creep modulus curves obtained for each series, using the parameters reported in Table 6. The creep modulus curves are, as expected, localized within the range of strains defined by the experimental results (see Fig. 12a–c). In Fig. 12d, all the obtained curves are overlaid in order to demonstrate that the adhesive of the three tested series exhibits similar shape of creep modulus curve. However, the creep modulus has a tendency to decrease with the age when the adhesive is prepared, indicating the occurrence of an

ageing effect on the adhesive constituents. Finally, it is worth mentioning that after 1000 h of loading, the creep modulus of the specimens decreased to 2.71 GPa, 2.37 GPa and 2.04 GPa, for Series I, II and III, respectively. Note that these reductions correspond to a decrease to 29%, 27% and 23% of the material's initial stiffness (taken as E_M). Unfortunately, none of the analysed papers either reported the full 1000 h period or an adhesive of similar stiffness in order to evaluate the significance of the obtained values.

4. Conclusions

This paper describes an experimental programme carried out aiming to characterize the tensile creep behaviour of an epoxy-based structural adhesive commonly used in NSM-CFRP strengthening applications. For that purpose, three series of tensile creep tests, composed of three adhesive samples per series, were executed. By taking the obtained results, the modified Burgers model was adjusted to the obtained experimental creep strain curves.

The obtained results showed that up to sustained stress levels of 60% of the adhesive's tensile strength, the adhesive can be assumed as a linear viscoelastic/viscoplastic material and parameterized using the modified Burgers model equation. Both the creep strain and creep modulus curves obtained using the modified Burgers equation exhibited very good agreement with the experimental results.

Furthermore, the obtained results provided a couple of qualitative observations. The first one is related to the level of strain experienced by the adhesive. While during material testing it was determined that the ultimate strain of the adhesive was about 3‰, when the tensile creep tests were performed, the adhesive endured 2 times that deformation level without rupturing. This fact demonstrates that after loaded, the adhesive is able of somehow reorganizing its internal structure to continuously withstand more and more deformation without rupturing. Another important remark is related to the observed loss of stiffness with the age of the adhesive container. The reduction of the values of the Kelvin components is notorious and, additional tests should be performed in order to confirm this tendency. Given this fact, and especially when the adhesive is intended for prestressed NSM-FRP, the time period between adhesive production and application should be carefully observed. This is a fundamental issue since the applied prestress level should remain as much as possible during the design life of the strengthening intervention (in general between 50 and 100 years). In this context, the occurrence of excessive creep can compromise the effectiveness of the prestressed NSM-CFRP technique that is being investigated under the framework of the present research project.

This experimental programme represents a first effort aiming to increase the knowledge on the creep of structural epoxy-based adhesives. However, much more research needs to be carried out, especially regarding the influence of the environmental conditions on the creep response.

References

[1] Barros JAO, Dias SJE, Lima JLT. Efficacy of CFRP-based techniques for the flexural and shear strengthening of concrete beams. Cem Concr Compos J 2007;29(3):203–17.
[2] Barros JAO, Dalfré GM. Assessment of the effectiveness of the embedded through-section technique for the shear strengthening of RC beams. Strain Int J 2013;49(1):75–93.
[3] De Lorenzis L, Teng JG. Near-surface mounted FRP reinforcement: an emerging technique for strengthening structures. Composites B 2007;38(2):119–43.
[4] Motavalli M, Czaderski C, Pfyl-Lang K. Prestressed CFRP for strengthening of reinforced concrete structures: recent developments at Empa, Switzerland. J Compos Constr 2011;15(2):194–205.
[5] El-Hacha R, Soudki K. Prestressed near-surface mounted fibre reinforced polymer reinforcement for concrete structures–a review. Can J Civ Eng 2013;40:1127–39.
[6] Quantrill RJ, Hollaway LC. The flexural rehabilitation of reinforced concrete beams by the use of prestressed advanced composite plates. Compos Sci Technol 1998;58(8):1259–75.
[7] Nordin H, Täljsten B. Concrete beams strengthened with prestressed near surface mounted CFRP. J Compos Constr 2006;10(1):60–8.
[8] Wang W-W, Dai J-G, Harries KA, Bao Q-H. Prestress losses and flexural behavior of reinforced concrete beams strengthened with posttensioned CFRP sheets. JCompos Constr 2012;16(2):207–16.
[9] ISO 899-1. Plastics—determination of creep behaviour—Part 1: tensile creep. Geneva, SZ: International Organization for Standardization (ISO); 2003.
[10] ASTM 2990. Standard test methods for tensile, compressive, and flexural creep and creep-rupture of plastics. Pennsylvania, US: American Society for Testing and Materials (ASTM); 2001. p. 20.
[11] Dean G. Modelling non-linear creep behaviour of an epoxy adhesive. Int J Adhes Adhes 2007;27(8):636–46.
[12] Feng CW, Keong CW, Hsueh YP, Wang YY, Sue HJ. Modeling of long-term creep behavior of structural epoxy adhesives. Int J Adhes Adhes 2005;25(5):427–36.
[13] Brinson HF, Brinson LC. Polymer Engineering Science and Viscoelasticity: An Introduction. New York, US: Springer Science+Business Media, LLC; 2008.
[14] Majda P, Skrodzewicz J. A modified creep model of epoxy adhesive at ambient temperature. Int J Adhes Adhes 2009;29(4):396–404.
[15] ISO 527-2. Plastics—determination of tensile properties—Part 2: test conditions for moulding and extrusion plastics. Geneva, SZ: International Organization for Standardization (ISO); 1993. p. 8.